uc3m | Universidad Carlos III de Madrid

e-Archivo

This is a postprint version of the following published document:

Serrano, D., Sánchez-Delgado, S., and Horvat, A. (2017). Effect of sepiolite bed material on gas composition and tar mitigation during C. cardunculus L. gasification. *Chemical Engineering Journal*, 317, 1037-1046

DOI: https://doi.org/10.1016/j.cej.2017.02.106

© Elsevier, 2017

This work is licensed under a Creative Commons Attribution-NonCommercial-NoDerivatives 4.0 International License.

Effect of sepiolite bed material on gas composition and tar mitigation during *C. cardunculus* L. gasification

Daniel Serrano[a,*], Sergio Sánchez-Delgado[a], Alen Horvat[b]

[a] *Energy Systems Engineering Research Group, Thermal and Fluid Engineering Department, Carlos III University of Madrid, Leganés (Madrid), Spain*
[b] *Carbolea Research Group, Department of Chemical and Environmental Sciences, University of Limerick, Limerick, Ireland*

Abstract

Sepiolite, a clay mineral that is commonly used as adsorbent, is proposed as bed material for biomass gasification in a lab-scale bubbling fluidized bed. In order to compare the obtained gas composition and tar generation, silica sand has been used as reference bed material. *C. cardunculus* L. has been employed as biomass feedstock. The operating temperature is varied from 830 to 875 °C, at constant equivalence ratio (ER) of 0.30. The gas produced with sepiolite as bed material has a slightly lower quality than the gas generated with silica sand, the lower heating value (LHV) is 0.4-1.4 MJ/Nm^3 lower for sepiolite than for silica sand. However, the tar generation is rather reduced in the sepiolite bed and the tar composition is also different among the bed materials: the polycyclic aromatic hydrocarbons fraction (PAH) is drastically reduced while oxygenated compounds arise in the sepiolite tests. Sepiolite properties such as surface area and morphology have been analysed by means of specific surface area (BET) and scanning electron microscopy (SEM-EDS) before and after the experiments. The fuel behaviour and the properties of sepiolite induce the adsorption of tars and molten ashes on the sepiolite surface, leading to a much better performance in terms of tar mitigation and agglomeration.

Keywords: sepiolite, *C. cardunculus* L., biomass, gasification, fluidized bed, tar

1. Introduction

Nowadays, global warming is an important environmental problem due to the huge amounts of energy demand by the developed society. As a consequence, there is an urgent need to reduce the greenhouse emissions and the dependence of fossil fuels to generate energy. In this sense, biomass gasification can provide a solution to this problem as its net contribution to the CO_2 emissions to the atmosphere is zero. However, the generation of a thick, black and highly viscous liquid called tar is a major issue in this technology. This element condenses on those surfaces that have low temperatures leading to the clogging

*Corresponding author. Tel:+34 91 624 8884
Email address: daserran@ing.uc3m.es (Daniel Serrano)

and a reduction in the performance of the different downstream equipments, the formation of tar aerosols or the polymerization into more complex structures that can cause unscheduled shut downs of the gasification plant. As a consequence, tars are a major barrier for biomass gasification commercialization [1, 2].

Different materials are commonly employed to reduce the tar content in the product gas: metal based catalysts, alkali based catalysts and natural occurring catalysts [3]. The first two groups are more expensive than natural ones and can be deactivated due to coke deposition or can cause agglomeration problems. Natural occurring materials such as dolomite has been reported as an effective tar reduction material although it lacks from a proper mechanical resistance towards attrition [4, 5]. Olivine and magnesite are other natural materials that reduces the amount of tars, not so effectively as dolomite but with a much higher mechanical resistance [2, 6, 7]. The use of alkali feldspars, bauxite, limestone, activated carbon or ilmenite have also been reported as effective tar reduction materials [8–13]. All these materials can be employed as bed materials in fluidized bed gasification or as an additives in different proportions.

A different type of natural materials such as porous clays can be also interesting bed materials or additives to reduce the tar content in the product gas from biomass gasification. The high porous structure and specific surface area help to crack heavy hydrocarbons obtaining a cleaner and better gas quality [14]. These materials have been used as oil-spill and dyes adsorbents from surfaces and waste water effluents [15, 16]. Natural occurring clays have been studied for pyrolysis and gasification applications [17–21]. All these studies agree that porous materials such as sepiolite, zeolite or bentonite, with a high pore structure and surface area, enhance the adsorption of tar and alkali content as well as they promote tar cracking reactions. These works are usually carried out under pyrolysis conditions (oxygen free and at lower temperatures than in gasification) using different facilities: fluidized beds, TGA and horizontal furnaces. However, there is rather limited literature using these materials in bubbling fluidized bed gasifiers.

In this work, sepiolite, a natural occurring clay ($Mg_8Si_12O_30(OH)_4(OH_2)_48H_2$) and with Spain as the largest producer (about 95 % of the world's annual production in the last decade [22]), is proposed as an alternative bed material to silica sand due to its adsorbent properties, chemical and mechanical stability and high surface area ($\sim$300 m^2/g) [15, 16, 23]. In previous works, the performance of sepiolite towards bed agglomeration has been investigated, obtaining higher defluidization times than operating with silica sand as bed material. In this case, sepiolite is tested and compared to silica sand under gasification conditions in a fluidized bed using *C. cardunculus* L. as biomass feedstock. Gas and tar composition are evaluated as well as the gasification performance for both silica sand and sepiolite. In order to test the adsorption properties of sepiolite towards tar generation, BET surface and SEM-EDS analyses have been carried out on sepiolite after the experiments.

2. Experimental methodology

2.1. Materials

C. cardunculus L. or cardoon is used as biomass feedstock for the gasification tests. It is an herbaceous perennial energy crop typical from Mediterranean regions [24] with good properties for gasification due to its high volatile matter content content like other commonly used energy crops (miscanthus or reed canary grass) [25]. The use of cardoon as energy crop also has some benefits such as low nitrogen and water demands, enhancement of soil characteristics or the use of lands that are not suitable for food production [24, 26]. Different equipments have been used to characterize this biomass (thermogravimetric and CHN analysers, and isoperibolic calorimeter). The elemental and proximate analyses of cardoon are shown in Table 1.

Table 1: *C. cardunculus* L. characterization.

Proximate analysis [wt.% ar]		*Ultimate analysis* [wt.% db]	
Moisture	7.03	Carbon	48.11
Volatile matter	72.29	Hydrogen	5.58
Fixed carbon[a]	15.01	Nitrogen	0.80
Ash	5.67	Oxygen[a]	39.42
High heating value [MJ/kg db]	17.80		

ar: as received, db: dry basis, [a] by difference

Biomass is received as cylindrical pellets of approximately 6 mm in diameter with lengths varying from 5 to 25 mm. In order to fulfil the feeding system requirements, the pellets are crushed prior to gasification into particles between 2.50 and 4.75 mm and bulk density of 442.82 ± 9.14 kg/m^3.

Silica sand supplied by INCUSA, Spain, and sepiolite supplied by TOLSA, Spain, are used as bed materials in separate experiments in order to check the sepiolite performance as bed material towards gas and tar compositions. Silica sand is commonly used bed material in fluidized bed gasification and, as a consequence, it is employed as reference material in this study. Both silica sand and sepiolite are sieved to between 425 and 600 μm. The minimum fluidization velocity (u_{mf}) is measured experimentally by means of pressure probes according with the procedure described by Kunii and Levenspiel [27]. u_{mf} is measured at 850 °C for the two bed materials prior to gasification. Taking into account the particle size and their respective densities both materials belong to type B materials according to Geldart′s classification [28]. Table 2 shows the main properties of the bed materials.

Table 2: Bed materials properties.

	Silica sand	Sepiolite
Density [kg/m^3]	2645	1551
Bulk density [kg/m^3]	1481	558
Mean particle diameter [μm]	512	512
Minimum fluidization velocity at 850 °C [m/s]	0.089	0.057

2.2. Experimental setup

The experiments are conducted in a lab-scale air-blown bubbling fluidized bed gasifier. Figure 1 shows a scheme of the facility. It consists of different sections: biomass feeding, air supply, fluidized bed reactor, cleaning section and product gas analysis. The feeding system section is composed by a vibrating cylinder in which a piston moves upwards and downwards inside the cylinder. The level of biomass particles is kept horizontal due to vibration and when these particles reached the discharge level, they fall down into the transfer tube towards the gasifier by its upper part. This tube is equipped with a water jacket to cool down the connection between the pipe and the reactor as well as to prevent biomass pyrolysis before it enters the reactor. A nitrogen flow is introduced into the feeding vessel in order to avoid backflow of gases from the gasifier. The fluidized bed reactor is a stainless steel 304 tube with an inner diameter of 52.8 mm. This tube is divided into two sections by a distributor plate with 38 orifices of 0.5 mm of inner diameter distributed in triangular pitch. The pressure drop across the perforate plate gives a value of $\Delta P_{dist} = 60440 \cdot u_g^2$ (at 850 ^{o}C). The whole reactor is surrounded by two electrical furnaces to provide the energy necessary to reach the desired temperature inside the bed and to simulate adiabatic conditions. The lower furnace acts as a gasifying agent preheater before it enters the bed.

The gas cleaning section is composed by a hot filter filled with glass wool which retains the entrained particles from the bed, a tar and water condenser, and cold filter for the remaining particles, tars and moisture. A solution of water and antifreeze agent circulates inside the condenser, cooling down the gas stream. The condensate, water and tars, are stored in a container at the bottom of the condenser. All the pipes from the gasifier to the condenser, including the hot filter are properly heated at 350 ^{o}C and isolated to prevent tar condensation before the condenser. The cold filter consists of three sections: a first section of cotton, a second section of cigarette filters, and a third section of silica gel.

Pressure is monitored in different parts of the facility: in the plenum (P_{plenum}), at 3 cm above the distributor plate (P_{3cm}) and before the hot filter (P_{filter}) by means of absolute pressure sensors (WIKA Type A-10, Honeywell SPT series and Kistler 4260A). Type K thermocouples are used to monitor temperature in the plenum (T_{plenum}), at 3 and 6 cm above the distributor plate (T_{3cm} and T_{6cm}), in the freeboard ($T_{freeboard}$), in the hot filter (T_{filter}), and in the condenser ($T_{condenser}$) (see Figure 1). The signals are collected using a National Instruments data acquisition modules: type 9205 (16 bit-resolution), type 9203 (16 bit-resolution) and type 9213 (24 bit-resolution) with analogue input channels, working at a sampling frequency of 400 Hz.

2.3. Experimental procedure

To perform the gasification experiments with silica sand and sepiolite, the bed is loaded with the bed material with a bed aspect ratio of $h_b/D = 2$ ($h_b = 105.6$ mm). This height is obtained using 342.50 g of silica sand or 129.10 g of sepiolite. The air supply is set to the experimental value. This air flow rate

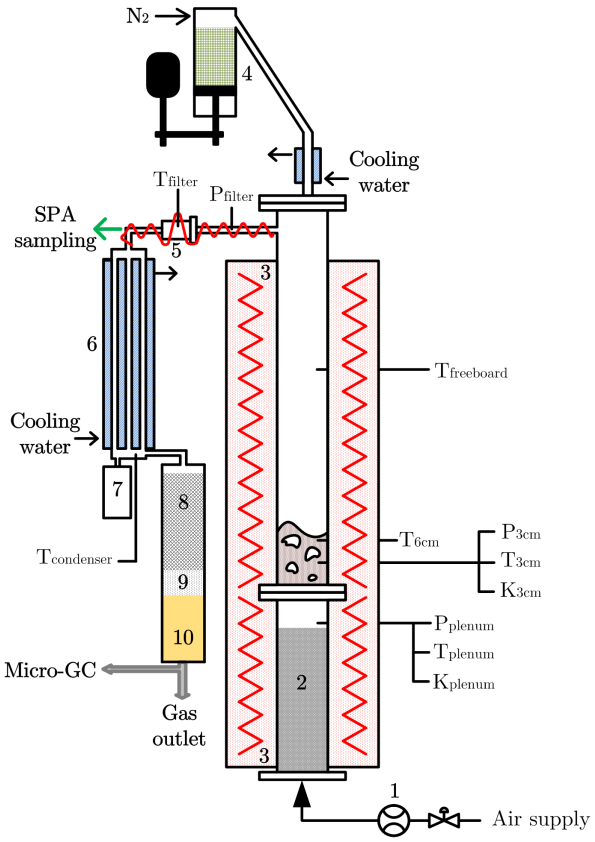

Figure 1: Scheme of the experimental facility: 1) mass flow meter; 2) air preheater; 3) electrical furnace; 4) vibrating biomass feeding system; 5) hot filter; 6) condenser; 7) water and tar trap; 8) cotton filter; 9) cigarette filters; 10) silica gel.

is chosen to obtain a $u/u_m f$ ratio of, approximately, 5. The selection of these parameters is based on a previous publication regarding the agglomeration phenomena [29]. The electrical furnaces are set depending on the bed material employed: in the case of sepiolite, the starting bed temperature is around 250 ^{o}C below the desired experimental temperature while in the case of silica sand, the starting bed temperature is quite close to the desired one. These differences in the plant operation are in relation with the combustible behaviour discussed in previous publications [29, 30]. The reactor takes around 90 minutes to get the initial temperatures to start biomass feeding.

Once the reactor temperatures are stable, biomass is introduced with a feeding rate corresponding to an ER = 0.3. The real ER is obtained after each experiment when the exact amount of biomass fed into the gasifier is known. This value is fixed to be in accordance with a previous work [29]. During the time needed to reach the steady state, around 30-40 minutes from the start of the biomass feeding, the furnace temperatures are adjusted to get the desired experimental temperature. A nitrogen flow of 0.5 Ndm^3/min is set from the feeding system to the reactor in order to prevent backflow of the product gases to the feeding

system. Table 3 summarizes the operating conditions for each experiment. The gasification temperature has been chosen the highest temperature inside the reactor since this temperature controls the gas and tar composition. In the case of silica sand, the highest temperature is obtained in the freeboard ($T_{freeboard}$) while for sepiolite, the highest temperature is measured inside the bed (T_{6cm}). This difference is motivated by the combustible behaviour as a consequence of the density ratio between bed material and biomass. The biomass tends to remain on the bed surface for silica sand bed while it tends to move inside the bed for sepiolite cases [29, 30]. As a consequence, the partial combustion of biomass, and thus, the highest temperature is obtained at different places inside the reactor.An example of the pressure and temperature profiles for one sepiolite experiment are shown in Figure 2.

Table 3: Operating conditions, syngas composition and gasification parameters from each gasification experiment.

Operating conditions				
Bed material [g]	silica sand	sepiolite	silica sand	sepiolite
	342.51	129.10	342.47	129.10
Biomass feeding rate [g_{daf}/h]	10.31	7.15	10.78	7.25
Biomass throughput [kg_{daf}/m^2h]	282.66	195.88	295.40	198.53
Air flow rate [Ndm^3/min]	15.25	10.50	15.25	10.50
ER [-]	0.30	0.30	0.29	0.29
Air excess ratio, u/u_{mf} [-]	4.69	5.21	4.90	5.39
T_{3cm} [^{o}C]	772.85	805.68	823.31	834.52
T_{6cm} [^{o}C]	784.30	827.83	832.82	873.50
$T_{freeboard}$ [^{o}C]	825.76	536.18	874.41	532.67
Dry syngas composition				
H_2 [% v/v]	8.64±0.38	9.00±0.71	10.97±0.28	8.17±0.82
CO [% v/v]	18.91±0.83	12.96±0.57	19.32±0.51	14.58±0.35
CH_4 [% v/v]	2.92±0.34	4.53±0.20	2.87±0.30	1.97±0.24
CO_2 [% v/v]	12.51±0.36	16.78±0.71	12.44±0.32	16.12±0.58
C_2H_4 [% v/v]	1.22±0.14	0.59±0.07	1.14±0.15	0.53±0.02
C_2H_6 [% v/v]	0.00±0.01	0.19±0.02	0.00±0.00	0.19±0.02
N_2 [% v/v]	55.80±1.65	55.84±1.58	53.27±1.27	58.45±1.85
H_2O [% v/v]	9.08	12.25	7.99	12.77
Gasification parameters				
Lower heating value [MJ/Nm^3]	5.07	4.70	5.31	3.86
Gas yield [$Nm^3/kg_{biomass\ daf}$]	2.17	2.19	2.17	2.07
Carbon conversion [%]	89.52	87.91	89.98	79.01
Hydrogen conversion [%]	43.29	52.38	49.10	34.23
Cold gas efficiency [%]	66.92	62.53	70.19	48.47
Elutriated fines [$g/kg_{biomass\ daf}$]	8.77	26.72	5.47	32.84
Moisture generation [$g/kg_{biomass\ daf}$]	173.96	245.26	151.70	242.86
GC detectable tar [$g/kg_{biomass\ daf}$]	21.76	11.11	22.52	9.22

2.4. Sampling and analysis

After leaving the reactor and passing through the cleaning section, the product gas is analysed every 3 minutes using an Agilent Micro-GC CP-4900 equipped with a thermal conductivity detector for the determination of permanent gases and light hydrocarbons. A Molsieve 5A column using argon as the carrier gas is employed for H_2, N_2, CH_4 and CO while a PPQ column using helium as the carrier gas is used for CO_2, C_2H_2, C_2H_4 and C_2H_6. Gas sampling is started at the same time as biomass feeding. The final gas

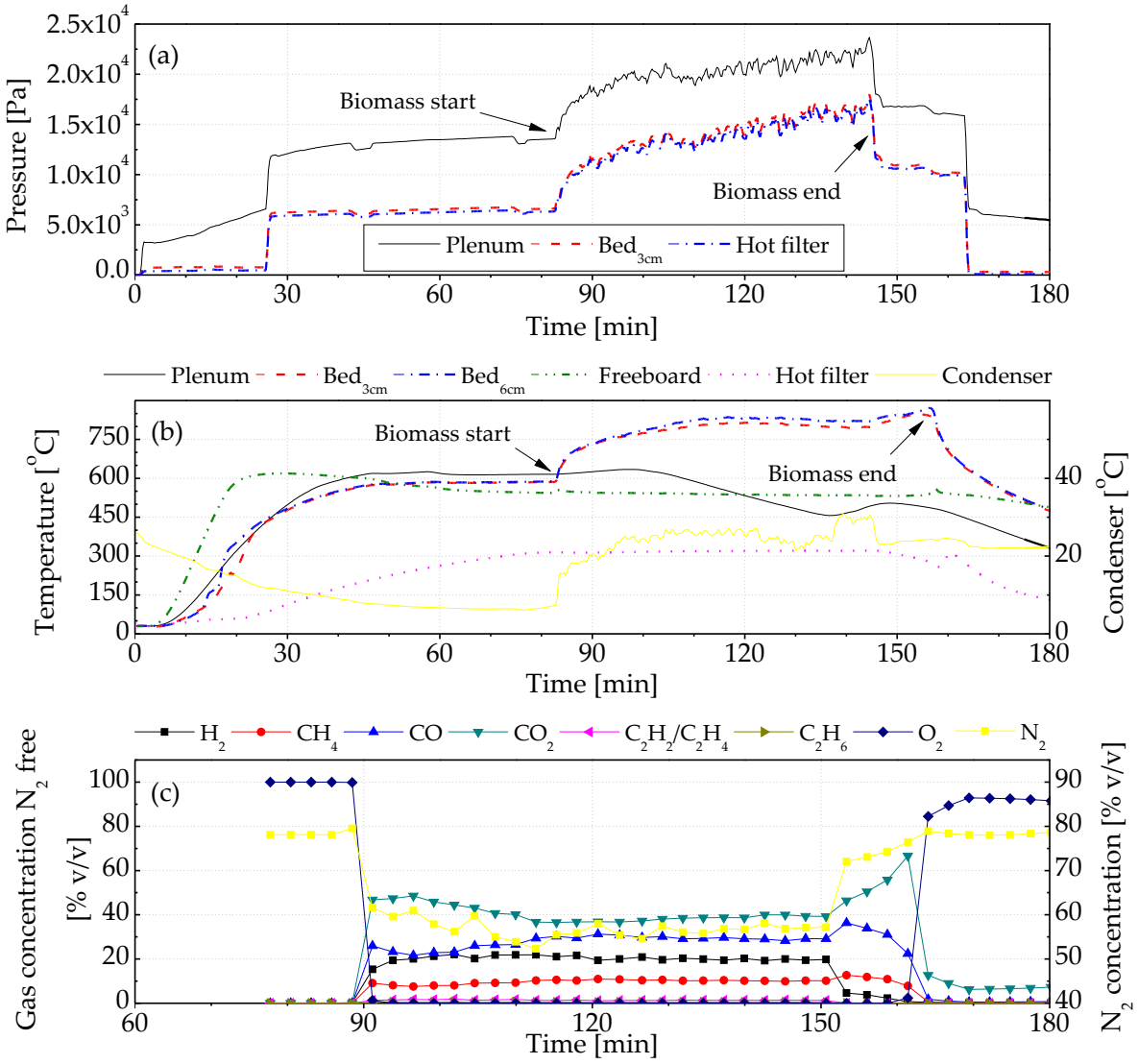

Figure 2: Pressure and temperature profiles for the experiments with sepiolite at 828 ^{o}C and ER = 0.30: a) pressure profiles, b) temperature profiles and c) gas profiles.

composition is calculated as the mean value during the steady state. This steady conditions are achieved 30-40 minutes after biomass feeding is started.

Solid Phase Adsorption method (SPA), developed by Brage et al. [31] and later modified by Osipovs et al. [32], is used for tar sampling. Different samples, at $\approx$ 350 ^{o}C, are taken manually during the steady state. These tar samples are taken from the SPA port placed between the hot filter and the condenser (see Figure 1). The SPA cartridges are extracted after each experiment using dichloromethane, and tert-butylcyclohexane and 4-ethoxyphenol are added as internal standards. A Varian 431-GC coupled to a Varian 210-MS (ion trap) are used for the analysis of the tar samples by GC-MS. Helium, with a constant flow rate of 1.2 ml/min,

is used as the carrier gas through a non-polar capillary column (VF-5MS). 1 μl is injected at 300 ^{o}C using an auto sampler in split mode 1:50. The GC oven is programmed as follows: initial temperature of 30 ^{o}C is kept for 5 minutes, then, temperature is raised to 180 ^{o}C with a heating rate of 5 ^{o}C/min, finally, 300 ^{o}C are obtained at a heating rate of 8 ^{o}C/min. The MS is configured with an automatic ionization energy, full scan mode (50-550 m/z mass range), 0.46 s/scan and a solvent delay of 2.10 minutes. The ion trap, manifold and transfer line are kept at 210, 60 and 300 ^{o}C, respectively. Tars identification, from benzene to chrysene, is performed with MassHunter software using the NIST 2.0 library. The quantification is carried out using the internal standards: phenols are quantified by means of the 4-ethoxyphenol/phenol calibration curve while the remaining tar compounds are quantified with the tert-butylcyclohexane/naphthalene calibration curve.

Tar results were calculated for normal conditions (NTP: 293.15 K and 101325 Pa). According to Siedlecki et al. [33] water vapour from the product gas condenses when passing through the sorbent, therefore, the sampled volume can be assumed to be taken on a dry basis (g/Nm^3 of raw dry gas converted further to g/kg$_{biomass\ daf}$). Final results are reported as the mean value for several samples and injections for each experiment, and they are presented as individual compounds as well as total GC detectable tar (referred as total tar henceforth and calculated as the sum of all identified species), secondary and tertiary tar groups as defined by Milne et al. [34].

After each experiment, the biomass hopper is discharged and weighted in order to get the real biomass feeding rate. The hot and cold filter, and the condenser are also cleaned. The filters are weighted before and after the experiment in order to get the mass of fines/condensates in these devices. Sepiolite bed material is analysed by means of BET surface area and SEM-EDS in order to check the changes in its properties associated to tar evolution.

Cold gas efficiency (CGE) defined as the energy input over the potential energy output (Eq. 1), carbon and hydrogen conversion defined as the ratio of carbon or hydrogen mass flow in the dry product gas to the mass flow rate of relevant the element in the dry and ash free biomass, lower heating value (LHV) of the product gas (Eq. 2, [1]), and the gas yield (GY) are calculated to evaluate the gasification performance. All the moisture from the product gas is assumed to be condensed out and collected in the condenser. The mean moisture generation rate is calculated dividing the weight of liquid collected in the condenser by the entire period of each gasification experiment, from the beginning of biomass feeding.

$$CGE = \frac{LHV \cdot GY}{\dot{m}_{fuel} \cdot LHV_{fuel}} \cdot 100 \tag{1}$$

$$\begin{aligned} LHV = &(10.78\ [\%v/v]_{H_2} + 12.63\ [\%v/v]_{CO} + 35.88\ [\%v/v]_{CH_4} + \\ &+ 64.34\ [\%v/v]_{C_2H_6} + 59.45\ [\%v/v]_{C_2H_4} + 56.07\ [\%v/v]_{C_2H_2})\ /100 \end{aligned} \tag{2}$$

3. Results and discussion

3.1. Gas composition

The gas composition obtained from the four gasification tests is shown in Figure 3 and Table 3. The use of one or another bed material has noticeable effect on the different species that form the product gas. The most significant differences appear on the CO, CO_2 and light hydrocarbons (C_2H_2, C_2H_4 and C_2H_6). The amount of CO and light hydrocarbons is relatively higher in the case of silica sand, while the CO_2 is rather higher for sepiolite. A feasible explanation for these differences in the gas composition is the effect of the combustible behaviour [30]. In the case of sepiolite, the biomass particles release the volatiles inside the bed and close to the air supply. These volatiles have to pass through the bed and the freeboard, and the oxygen molecules have more time for oxidation not only the char but also the CO and H_2 molecules, producing more CO_2 and H_2O. However, with silica sand, the volatiles are released on the top of the bed and goes directly to the freeboard where there is a more reducing atmosphere, generating more CO in detriment of CO_2 and H_2O. Xie et al. [19] found higher CO_2 concentration than CO using sepiolite under pyrolysis conditions. They referred a weaker catalytic role of sepiolite over gasification reactions ($C + CO_2 \leftrightarrow 2CO$ and $C + H_2O \leftrightarrow CO + H_2$) and cracking reactions (Tar $\rightarrow H_2 + CO + CO_2 +$ char $+ C_nH_m$ and $C_nH_m \rightarrow H_2 +$ char). Vesses et al. [21] also found similar results under pyrolysis conditions using silica sand and sepiolite. Besides, C_2H_6 only is detected in this latter case, when sepiolite is used as bed material. The higher production of C_2H_2 and C_2H_4 in silica sand might be due to the tar cracking [36] as well as from the aromatic compounds of these tars [35]. Tars released from the biomass particles, when silica sand is used, goes directly to the freeboard where the temperature is higher, enhancing the cracking reactions. However, in the case of sepiolite, the tars are partially generated on the bed surface. These tars goes to the freeboard where the temperature is not so high to promote the cracking reactions.

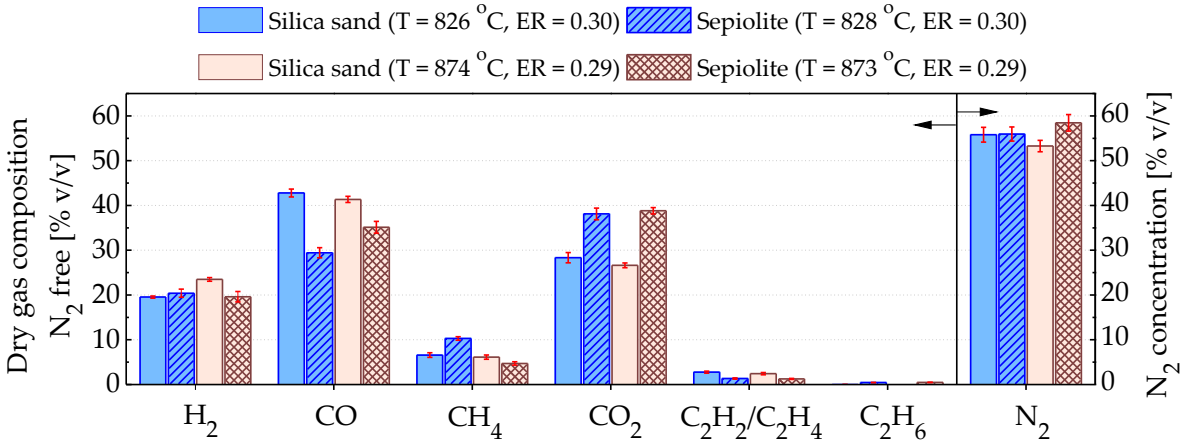

Figure 3: Gas composition (dry and N_2 free) for silica sand and sepiolite at different temperatures and ER.

As it can be observed, there is not a clear trend in the gas composition with temperature for silica sand and sepiolite. In the case of silica sand, a bit higher H_2 amount is obtained when increasing temperature from 826 to 874 °C while a higher CO and lower CH_4 concentrations are observed for sepiolite. These trends are in agreement with the literature [35, 37, 38] although its effect is not very significant due to the small range of temperature evaluated.

The product gas ratios are shown in Figure 4. The CO/CO_2 ratio is higher in the case of silica sand for both experimental conditions. This means that the Boudouard reaction ($C + CO_2 \leftrightarrow 2CO$) is promoted when silica sand is employed as bed material. The H_2/CO ratio is a bit higher for sepiolite at 827 ^oC and similar to silica sand at 874 ^oC, indicating that the water-gas shift reaction ($CO + H_2O \leftrightarrow H_2 + CO_2$) has smaller influence than the Boudouard reaction. Regarding the H_2/CO_2 and the CH_4/H_2 ratios which give information about the dry reforming reaction ($C_nH_m + nCO_2 \leftrightarrow (m/2)H_2 + 2nCO$), the former is higher in silica sand experiments while the latter is higher in sepiolite experiments at 830 °C and similar to silica sand at 874 °C. This indicates that the dry reforming reaction is enhanced in the silica sand tests.

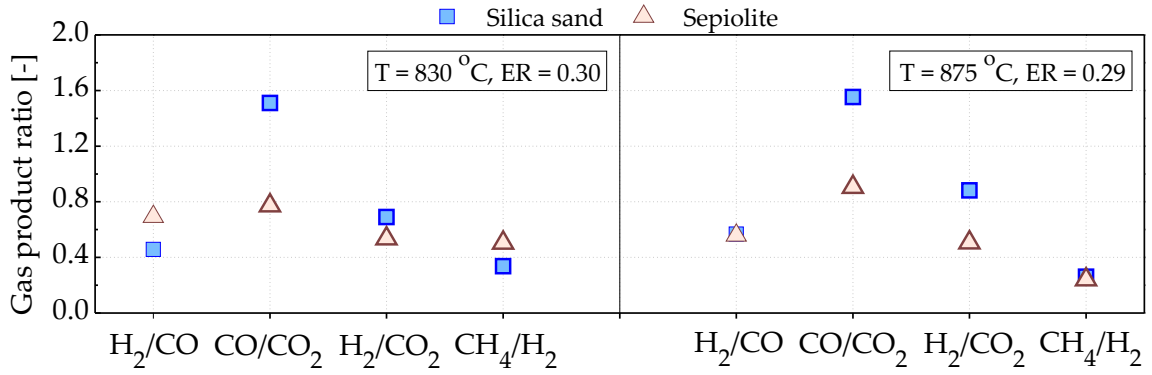

Figure 4: Gas composition (dry and N_2 free) for silica sand and sepiolite at different temperatures and ER.

The use of sepiolite does not increase the H_2 or CO concentration in the product gas in comparison with the results obtained using silica sand as bed material. Similar results have been reported by Veses et al. [21] using silica sand and sepiolite under pyrolysis conditions in an auger reactor. On the other hand, Noda et al. [20] only obtained a slightly higher H_2 concentration in the gas due to the use of acidified bentonite.

3.2. Gasification performance

In order to evaluate the gasification performance, both C and H conversion, the CGE, the GY and the LHV of the produced gas are calculated. Figure 5 and Table 3 show the results of these calculations. Carbon conversion is higher for silica sand than for sepiolite as a consequence of the higher CO, C_2H_2 and C_2H_4 quantities in the product gas, being this parameter between 79 and 90 % for all cases. Hydrogen conversion ranges between 34 and 53 %. In this case, the higher generation of H_2 and CH_4 for sepiolite at 827 ^oC gives a higher H conversion than for silica sand contrary to the experiments at 874 ^oC where the H conversion is

higher for silica sand due to the higher H_2 and CH_4 generation. The lower conversion of hydrogen in relation to carbon resides on the hydrogen losses due to the water, ammonia and hydrogen sulphide in the product gas. The LHV of the product gas is influenced by the gas composition as the gas species have different importance on the final value. The use of silica sand inside the bed generates a product gas with a higher energy content as a consequence of the higher CO and light hydrocarbons production. The differences are narrower at 827 ^{o}C because of the higher concentration of CH_4 in the sepiolite gas. The GY is very similar for all tested conditions and bed materials. The CGE evaluates the energy in the product gas in relation to the energy input from the biomass. This parameter is higher for silica sand than for sepiolite for both 827 and 874 ^{o}C, being the values between 48 and 70 %.

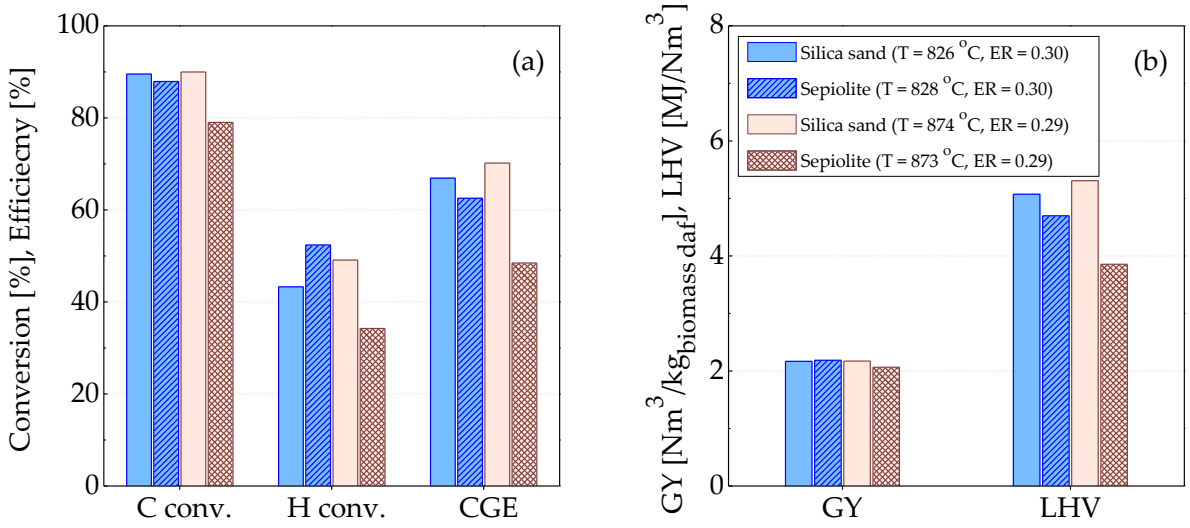

Figure 5: Gasification performance for silica sand and sepiolite at different temperatures and ER: a) C and H conversion, and CGE, and b) GY and LHV.

The amount of elutriated fines is lower in silica sand than in sepiolite (Table 3). This is in accordance with the high mechanical resistance of silica sand and the fines generated by abrasion in the case of sepiolite. The moisture generation shows also bigger values for sepiolite than for silica sand. The reason, as stated above, can be the better contact of the volatiles with the oxygen molecules inside the sepiolite bed, producing more H_2O and CO_2.

3.3. Tar composition

Figure 6 shows the tar quantities for the different tar groups: secondary (i.e.: benzene, toluene, phenol...), tertiary-alkyl (i.e.: 2-methylnaphthalene...) and tertiary-PAH (i.e.: naphthalene, fluorene, pyrene...), as well as total tar, quantified as the sum of all identified species, and BTEX (benzene, toluene, ethylbenzene and

xylenes). There are significant differences in the tar production depending on the bed material used. Using sepiolite, the total tar is reduced for about 50 % with respect to silica send at the same temperature and ER conditions. Tar reduction properties of sepiolite can also be observed in the presented tars groups. In the case of secondary tars, the tar reduction effect of sepiolite is not so high, increasing a little bit when temperature is incremented from 827 to 874 °C. However, this effect is not obvious since the quantities are within the margin of error. For tertiary-alkyl tars, sepiolite produces around a 50 % less compounds than silica sand. Nevertheless, the quantities of tertiary-alkyl tars are not as significant as for example for tertiary PAH tars. The highest tar reduction is observed in the tertiary-PAH group, where quantities decrease more than 90% (90.8 and 94.7% for 830 and 875 °C, respectively). The BTEX fraction is also around 60% lower for sepiolite than for silica sand, independently of the temperature. Thereby, good tar reduction activity of sepiolite, in particular to reduce tertiary-PAH and BTEX compounds, is responsible for the lower total tar content.

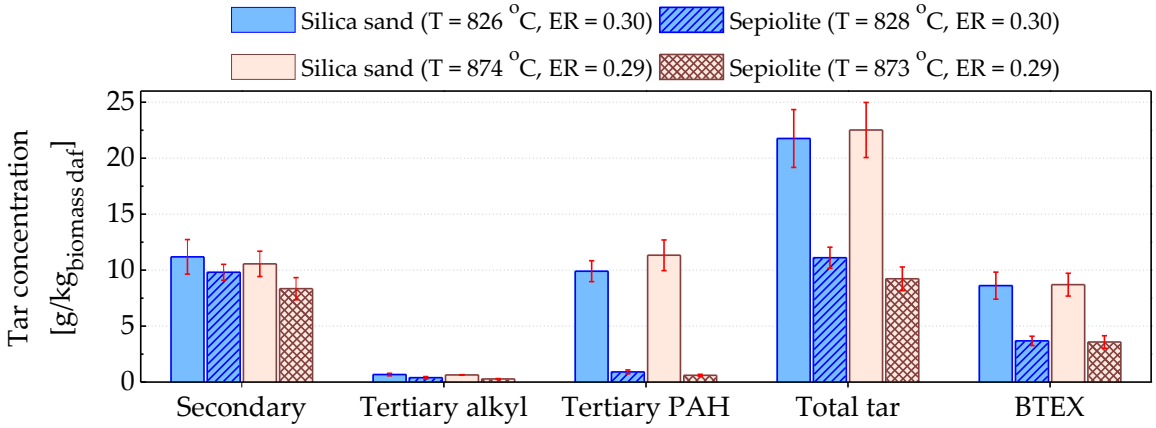

Figure 6: Tar concentration according to Milne et al. [34].

Figure 7 presents the tar composition for the 25 identified tar species and notable differences between two bed materials can be observed. The main tar species for silica sand are benzene, naphthalene, acenaphthylene and phenanthrene, while cresols, phenol, toluene and benzene are the most abundant tar compounds in sepiolite. Benzene and PAHs are drastically reduced with a sepiolite bed as it is shown in Figures 6 and 7. Chrysene (M $\approx$ 228.29 g/mol) is the heaviest tar compound identified when silica sand is used as a bed material, while anthracene (M $\approx$ 178.23 g/mol) is the heaviest tar compound identified during sepiolite gasification.

One of the most remarkable differences between silica sand and sepiolite is that phenols, ethylbenzene and xylenes are only present when sepiolite is used as bed material. This observation can be due to the combustible behaviour and the differences in the place where the highest temperature occurs as this parameter is one of the most relevant while explaining tar evolution. In the case of silica sand, with a higher

bulk density, the biomass particles float on the top of the bed. The contact between volatiles and the bed material is limited since the released volatiles migrate directly to the freeboard [40] where the temperature is higher than the bed temperature as the partial combustion of biomass does not take place inside the bed (see bed and freeboard temperatures in Table 3). The temperature in the freeboard is higher than 750 ^{o}C, and consequently, oxygenated species are converted into PAH via cyclopentadiene radicals which then combine to generate aromatics with two or more rings as sugessted by Fitzpatrick et al.[41] and Yu et al. [42]. On the other hand, with sepiolite as bed material, biomass particles are distributed inside the bed and also on the bed surface. The partial combustion of biomass occurs inside the bed increasing the temperature in this part of the reactor which is higher than in the freeboard (see Table 3). Volatiles are released inside the bed as well as on the top of the bed. Volatiles formed on the bed surface enter directly into the freeboard where the temperature is lower than 750 ^{o}C and hence, oxygenated tars are not reformed, remaining in the product gas. This explains why the secondary tars are not reduced in the same magnitude than BTEX or tertiary-PAH groups. Although benzene is highly reduced in the case of sepiolite, the occurrence of compounds such as xylenes or phenols, which are not present in the silica sand case, make this reduction not such high.

The presence of single ring alkyated tars and phenols in the sepiolite experiments can be explained by low freeboard temperature ($\approx$ 534 ˚C), limiting temperature reforming of secondary tars into tertiary aromatic tars. On the other hand, the larger number of PAHs as well as their larger quantities in the silica sand experiments ($T_{freeboard}$ = 874 ˚C) indicate promoted temperature reforming reactions in the freeboard. Since the mixing regime between biomass and the bed material is not the same, it cannot be justified to what extend the catalytic effect of the sepiolite and silica sand affect the tar reforming reactions.

3.4. Sepiolite analysis after gasification

Sepiolite is known to be a porous material with a high specific surface area, between $\approx$75 and $\approx$400 m^2/g [43]. The specific surface area can be also related with the tar reduction in the gasification process. The pores, cavities as well as the sepiolite surface can accommodate different tar molecules. Different studies have demonstrated the the capacity of sepiolite to adsorb oils [15], wastewater [16] and other elements such as water, benzene, pyridine, or ethylbenzene [44]. The results show that these compounds are mainly adsorbed on the surface of the sepiolite and a small amount are adsorbed in the internal cavities. This process highly decreases the specific surface area. In order to investigate if these effects are responsible of the differences obtained in the tar production and composition, fresh and used sepiolite have been analysed by employing BET surface area and SEM-EDS techniques.

The fresh sepiolite employed in the experiments results in a BET surface area of 199.2 m^2/g. This value agrees with the BET surface areas reported in the literature [43, 45]. In the case of used sepiolite, after the cardoon gasification, the BET surface area is reduced to 6.5 m^2/g. This reduction might has two

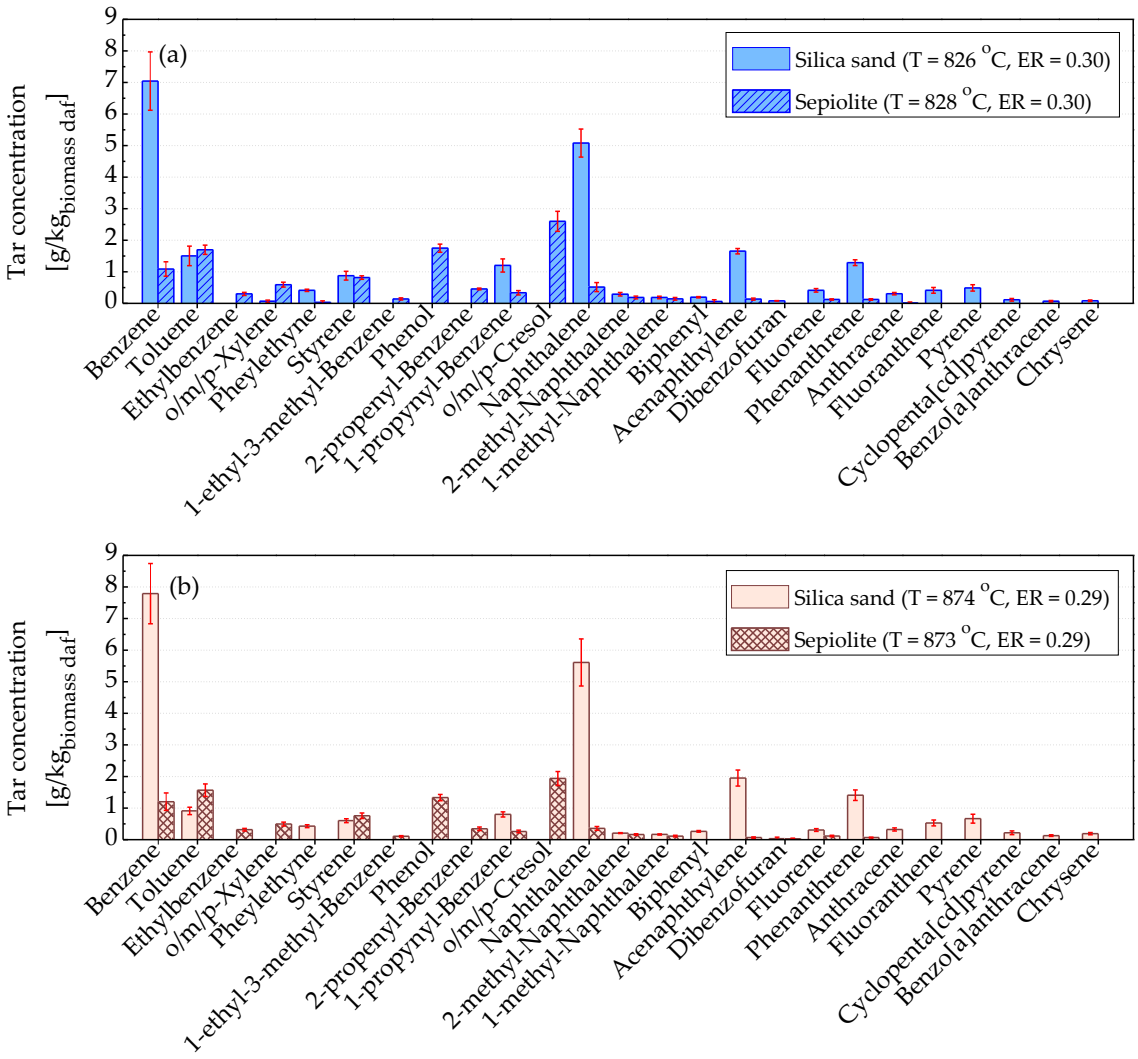

Figure 7: Tar concentration for individual compounds for both silica sand and sepiolite: a) T = 827 ^{o}C and ER = 0.30 and b) T = 874 ^{o}C and ER = 0.29.

contributions: a change in the internal structure of the sepiolite due to the heating above 350 °C [46–48], and the adsorption of different compounds on the sepiolite surface. Ito et al. [17] also experimented a decrease in the BET surface area of sepiolite after tar capture at pyrolysis conditions.

Figure 8 shows the SEM images of fresh and used sepiolite. Some differences between the two figures can be noticed. Fresh sepiolite (Figure 8a) shows a lot of fibres that are completely transformed after cardoon gasification (Figure 8b). Rounded grains can be observed after the experiments which might indicate a possible deposits of molten ashes and tars on the surface of sepiolite.

Table 4 shows the results of the SEM-EDS analysis. Fresh sepiolite is formed by oxygen, magnesium, aluminium silicon and chlorine. However, the composition of the used sepiolite is quite different. Two zones are distinguished in this second case: a smooth zone (spectrums 1 and 3) and a rough zone (spectrums 2 and

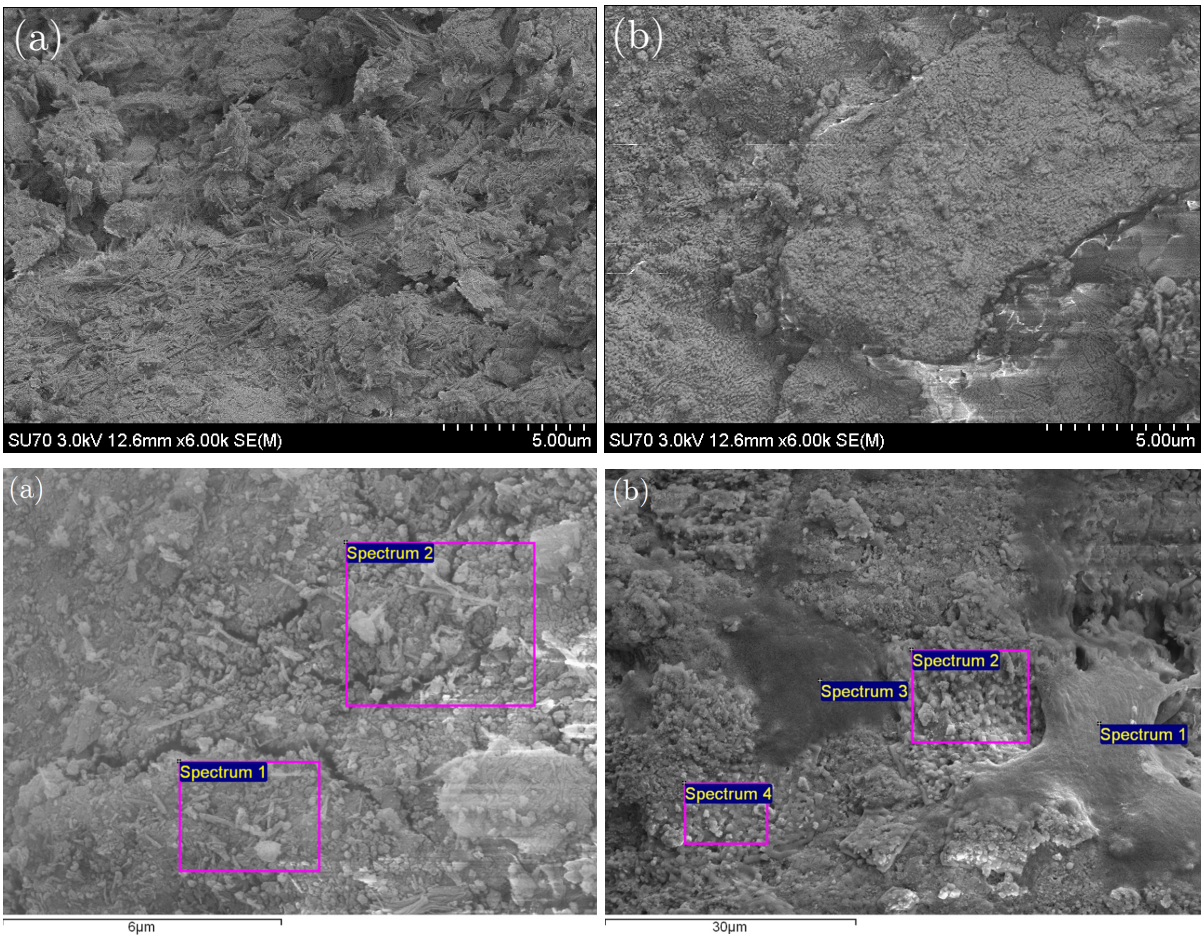

Figure 8: SEM analysis for sepiolite: a) fresh sepiolite and b) used sepiolite.

4). Looking into the composition of the smooth zone, a high amount of carbon is observed with very small quantities of other minor elements. This carbon may comes from the adsorbed tars on the surface of the sepiolite. The rough zone shows no or minor amounts of carbon and high quantities of elements typical from biomass ashes such as Na, Cl, K and Ca. These results confirm the hypothesis of adsorbed tars, obtaining a cleaner gas. This results were also confirmed by Ito et al. [17] who referred that micropores in the sepiolite are plugged by tar hydrocarbons and capture tar. Besides, they also show that molten ashes are adsorbed on the surface, avoiding agglomeration problems.

In addition, a solvent extraction with dichloromethane has been performed in sample of sepiolite after gasification. The extracted compounds have been analysed by GC-MS to get an indication of the possible adsorbed tars. Figure 9 shows the chromatogram of this analysis. Peaks for naphthalene, acenaphthylene, dibenzofuran, fluorene and phenanthrene can be observed, supporting the above hypothesis that sepiolite adsorbs the tars generated in the bed. This result is also in agreement with the low tertiary-PAH tars generated in the product gas as they are adsorbed by the sepiolite.

Table 4: Identified species from SEM-EDS analysis on fresh and used sepiolite.

	C	O	Mg	Al	Si	Cl	Na	K	Ca
Fresh sepiolite [wt.%]									
Spectrum 1		58.08	10.61	2.75	26.76	1.81			
Spectrum 2		58.33	12.56	2.41	25.76	0.95			
Used sepiolite [wt.%]									
Spectrum 1	75.54	22.70					1.77		
Spectrum 2	11.64	15.08	3.75	0.92	1.46	34.23	14.83	14.85	3.25
Spectrum 3	61.47	28.30	2.87	0.51	2.36		0.96		3.55
Spectrum 4		13.90	1.45	0.87	1.34	41.99	18.21	19.49	2.75

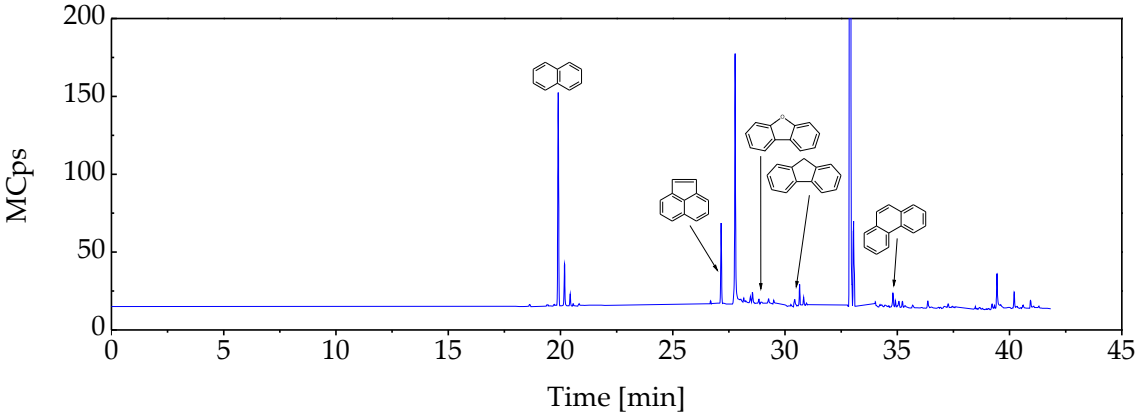

Figure 9: Total ion current chromatogram from GC/MS for the adsorbed tars in the used sepiolite

4. Conclusions

In this work, sepiolite has been tested under gasification conditions in terms of gas and tar composition, comparing the results with a commonly used bed material like silica sand.

The use of sepiolite do not improve the gas composition, generating more CO_2 and less CO than the gas produced by silica sand while the H_2 content does not show a clear trend between the two bed materials. The carbon conversion, CGE and LHV of the raw gas are also smaller in the case of sepiolite as bed material.

In relation to the tar generation, sepiolite efficiently reduces the tar generation up to 50% in comparison with silica sand, and specifically sepiolite reduces the tertiary-PAH tars. The composition of these tars is also quite different, appearing single ring alkyated and oxygenated compounds such as xylenes and phenols in sepiolite, and disappearing tars with a molecular weight higher than anthracene.

The high reduction of tars in the product gas is achieved due to the physical properties of sepiolite: porous structure and high surface area that adsorb the tar compounds on its surface, mainly tertiary-PAH compounds, as well as the molten ashes, reducing the risk of agglomeration.

Acknowledgments

The authors would like to express their gratitude to the financial support of the Spanish Ministry of Economy and Competitiveness from project ENE2014-54942-R. The authors also would like to thank Yina Guo who performed SEM-EDS analyses and to Lidia Muñoz who carried out BET analyses.

Alen Horvat acknowledges COST funding (short term scientific mission-STSM) under a COST STSM Reference Number: COST-STSM-FP1306-34300, supporting his exchange stay at University Carlos III of Madrid.

References

[1] Basu P. Biomass Gasification and Pyrolysis: Practical Design and Theory. Amsterdam: Elsevier Inc.; 2010.

[2] Siedlecki M, Nieuwstraten R, Simeone E, de Jong W, Verkooijen HM. Effect of magnesite as bed material in a 100 kW_{th} steam–oxygen blown circulating fluidized–bed biomass gasifier on gas composition and tar formation. Energy & Fuels 2009;23:5643–5654.

[3] Alauddin ZABZ, Lahijani P, Mohammadi M, Mohamed AR. Gasification of lignocellulosic biomass in fluidized beds for renewable energy development: a review. Renewable and Sustainable Energy Reviews 2010;14:2852-2862.

[4] Berrueco C, Montane D, Guell BM, Alamo G. Effect of temperature and dolomite on tar formation during gasification of torrefied biomass in a pressurized fluidized bed. Energy 2014;66:849-859.

[5] Rapagnà S, Jand N, Kiennemann A, Foscolo PU. Steam–gasification of biomass in a fluidised–bed of olivine particles. Biomass & Bioenergy 2000;19:187-197.

[6] Corella J, Toledo JM, Padilla R. Olivine or dolomite as in–bed additive in biomass gasification with air in a fluidized bed: which is better? Energy & Fuels 2004;18:713-720.

[7] Thakkar M, Makwana JP, Mohanty P, Shah M, Singh V. In bed catalytic tar reduction in the autothermal fluidized bed gasification of rice husk: Extraction of silica, energy and cost analysis. Industrial Crops and Products 2016;87:324–332.

[8] Berguerand N, Marinkovic J, Vilches TB, Thunman H. Use of alkali–feldspar as bed material for upgrading a biomass–derived producer gas from a gasifier. Chemical Engineering Journal 2016;295,80–91.

[9] Vilches TB, Marinkovic J, Seemann M, Thunman H. Comparing Active Bed Materials in a Dual Fluidized Bed Biomass Gasifier: Olivine, Bauxite, Quartz–Sand, and Ilmenite. Energy & Fuels 2016;30:4848–4857.

[10] Pandey DS, Kwapinska M, Gómez-Barea A, Horvat A, Fryda LE, Rabou LPLM, Leahy JJ, Kwapinski W. Poultry Litter Gasification in a Fluidized Bed Reactor: Effects of Gasifying Agent and Limestone Addition. Energy & Fuels 2016;30:3085–3096.

[11] Choi YK, Cho MH, Kim JS. Air gasification of dried sewage sludge in a two–stage gasifier. Part 4: Application of additives including Ni–impregnated activated carbon for the production of a tar–free and H_2–rich producer gas with a low NH_3 content. International Journal of Hydrogen Energy 2016;41:1460–1467.

[12] Larsson A, Israelsson M, Lind F, Seemann M, Thunman H. Using Ilmenite To Reduce the Tar Yield in a Dual Fluidized Bed Gasification System. Energy & Fuels 2014;28:2632–2644.

[13] Campoy M, Gómez-Barea A, Fuentes-Cano D, Ollero P. Tar Reduction by Primary Measures in an Autothermal Air-Blown Fluidized Bed Biomass Gasifier. Industrial & Engineering Chemistry Research 2010;49:11294–11301.

[14] Sun Y, Li R, Yang T, Kai X, He Y. Gasification of biomass to hydrogen–rich gas in fluidized beds using porous medium as bed material. International Journal of Hydrogen Energy 2013;38:14208–14213.

[15] Zadaka-Amir D, Bleiman N, Mishael YG. Sepiolite as an effective natural porous adsorbent for surface oil-spill. Microporous and Mesoporous Materials 2013;169:153–159.

[16] Dogan M, Ozdemir Y, Alkan M. Adsorption kinetics and mechanism of cationic methyl violet and methylene blue dyes onto sepiolite. Dyes and Pigments 2007;75:701–713.

[17] Ito K, Moritomi H, Yoshiie R, Uemiya S, Nishimura M. Tar capture effect of porous particles for biomass fuel under pyrolysis conditions. Journal of Chemical Engineering of Japan 2003;36: 840–845.

[18] Namioka T, Yoshikawa K, Hatano H, Suzuki Y. High tar reduction with porous particles for low temperature biomass gasification: effects of porous particles on tar and gas yields during sawdust pyrolysis. Journal of Chemical Engineering of Japan 2003;36:1440–1448.

[19] Xie YR, Shen LH, Xiao J, Xie DX, Zhu J. Influences of additives on steam gasification of biomass. 1. Pyrolysis procedure. Energy & Fuels 2009;23:5199–5205.

[20] Noda R, Ito T, Tanaka N, Horio M. Steam gasification of cellulose and wood in a fluidized bed of porous clay particles. Journal of Chemical Engineering of Japan 2009;42:490–501.

[21] Vesses A, Aznar M, López JM, Callén MS, Murillo R, García T. Production of upgraded bio–oils by biomass catalytic pyrolysis in an auger reactor using low cost materials. Fuel 2015;141:17–22.

[22] Murray HH, Pozo M, Galán E. An introduction to palygorskite and sepiolite deposits – Location, geology and uses. In Developments in Palygorskite-Sepiolite Research 2011.

[23] Pecharromán C, Esteban-Cubillo A, Montero I, Moya JS. Monodisperse and corrosion-resistant metallic nanoparticles embedded into sepiolite particles for optical and magnetic applications. Journal of the American Ceramic Society 2006;89:3043-3049.

[24] Fernández J, Curt MD. State of the art of *Cynara Cardunculus* L. as an energy crop. In: Sjunnesson L, Carrasco JE, Helm P, Grassi A, editors. 14^{th} European Conference and Technology Exhibition on Biomass Energy, Industry and Climate Protection, Paris: ETA-Renewable Energies and WIP Renewable Energies; 2005:22-27.

[25] Phyllis2 database for biomass and waste. https://www.ecn.nl/phyllis2. Energy research Centre of the Netherlands

[26] Grammelis P, Malliopoulou A, Basinas P, Danalatos NG. Cultivation and characterization of Cynara Cardunculus for solid biofuels production in the Mediterranean region. International Journal of Molecular Sciences 2008;9:1241-1258.

[27] Kunii D, Levenspiel O. Fluidization engineering. 2nd edn. Butterworth-Heinemann; 1991.

[28] Geldart D. Types of Gas Fluidization. Powder 1973;7:285-292.

[29] Serrano D, Sánchez-Delgado S, Sobrino C, Marugán-Cruz C. Defluidization and agglomeration of a fluidized bed reactor during *Cynara cardunculus* L. gasification using sepiolite as a bed material. Fuel Processing Technology 2015;131:338–347.

[30] Gómez-Hernández J, Serrano D, Soria-Verdugo A, Sánchez-Delgado S. Agglomeration detection by pressure fluctuation analysis during *Cynara cardunculus* L. gasification in a fluidized bed. Chemical Engineering Journal 2016;284:640–649.

[31] Brage C, Yu Q, Chen G, Sjöström K. Use of amino phase adsorbent for biomass tar sampling and separation. Fuel 1997;76:137-142.

[32] Osipovs S. Comparison of efficiency of two methods for tar sampling in the syngas. Fuel 2013;103:387–392.

[33] Siedlecki M, de Jong W. Biomass gasification as the first hot step in clean syngas production process - gas quality optimization and primary tar reduction measures in a 100 kW thermal input steam-oxygen blown CFB gasifier. Biomass Bioenergy 2011;35:S40-S62.

[34] Milne TA, Evans RJ, Abatzoglou N. Biomass Gasifier "Tars": Their Nature , Formation and Conversion. National Renewable Energy Laboratory, NREL/TP–570–25357; 1998.

[35] Narváez I, Orío A, Aznar MP, Corella J. Biomass gasification with air in an atmospheric bubbling fluidized bed. Effect of six operational variables on the quality of the produced raw gas. Industrial & Engineering Chemistry Research 1996;35:2110–2120.

[36] Azhar Uddin MD, Tsuda H, Wu S, Sasaoka E. Catalytic decomposition of biomass tars with iron oxide catalysts. Fuel 2008;87:451–459.

[37] de Andrés JM, Narros A, Rodríguez ME Behaviours of dolomite, olivine and alumina as primary catalysts in air-steam gasification of sewage sludge. Fuel 2011;90:521–527.

[38] Mohammed MAA, Salmiaton A, Wan Azlina WAKG, Mohammed Amran MS, Fakhru'l-Razi A. Air gasification of empty fruit bunch for hydrogen–rich gas production in a fluidized-bed reactor. Energy Conversion and Management 2011;52:1555–1561.

[39] Christodoulou C, Tsekos C, Tsalidis G, Fantini M, Panopoulos KD, de Jong W, Kakaras E. Attempts on cardoon gasification in two different Circulating fluidized Beds. Case Studies in Thermal Engineering 2014;4:42–52.

[40] Mayerhofer M, Fendt S, Spliethoff H, Gaderer M. Fluidized bed gasification of biomass – In bed investigation of gas and tar formation. Fuel 2014;117:1248–1255.

[41] Fitzpatrick EM, Jones JM, Pourkashanian M, Ross AB, Williams A, Bartle KD. Mechanistic aspects of soot formation from the combustion of pine wood. Energy Fuels 2008;22:3771–3778.

[42] Yu H, Zhang Z, Li Z, Chen D. Characteristics of tar formation during cellulose, hemicellulose and ligning gasification. Fuel 2014;118:250–256.

[43] Suárez M, García-Romero E. Variability of the surface properties of sepiolite. Applied Clay Science 2012;67–68:72–82.

[44] Inagaki S, Fukushima Y, Doi H, Kamigaito O. Pore size distribution and adsorption selectivity of sepiolite. Clay Minerals 1990;25:99–105.

[45] Sánchez-Martín MJ, Rodríguez-Cruz MS, Andrabes MS, Sánchez-Camazano M. Efficiency of different clay minerals modified with a cationic surfactant in the adsorption of pesticides: Influence of clay type and pesticide hydrophobicity. Applied Clay Science 2006;31:216–228.

[46] Serna C, Ahlrichs JL, Serratosa JM. Folding in sepiolite crystals. Clays and Clay Minerals 1975;23:452–457.

[47] Balci S. Thermal decomposition of sepiolite and variations in pore structure with and without acid pre-treatment. Journal of Chemical Technology and Biotechnology 1996;66:72–78.

[48] Balci S. Effect of heating and acid pre-treatment on pore size distribution of sepiolite. Clay Minerals 1999;34:647–655.

Abbreviations

BTEX benzene, toluene, ethylbenzene and xylene

CGE cold gas efficiency

daf dry-ash free

ER equivalent ratio

GC gas chromatoghraphy

GY gas yield

LHV lower heating value

MS mass spectrum

NTP normal temperature and pressure conditions

PAH polyaromatic hydrocarbons

SPA solid phase adsorption

Supplementary data

Table 5: Identified and quantified tar compounds in g/Nm$^3_{raw\ gas}$.

Tar compound	Retention time [min]	Tar group[a]	Silica sand T = 826 ˚C ER = 0.30	Sepiolite T = 828 ˚C ER = 0.30	Silica sand T = 873 ˚C ER = 0.29	Sepiolite T = 874 ˚C ER = 0.29
Benzene	3.23	secondary	3.25±0.43	0.50±0.10	3.59±0.44	0.58±0.13
Toluene	6.42	secondary	0.69±0.14	0.78±0.07	0.42±0.05	0.76±0.10
Ethylbenzene	10.31	secondary	0.00	0.14±0.02	0.00	0.15±0.01
o/m/p-Xylene	10.68	secondary	0.03±0.02	0.27±0.04	0.00	0.24±0.03
Phenylethyne	10.94	secondary	0.19±0.02	0.01±0.02	0.20±0.02	0.00
Styrene	11.56	secondary	0.41±0.06	0.37±0.03	0.28±0.03	0.37±0.04
1-ethyl-3-methyl-Benzene	14.18	secondary	0.00	0.06±0.02	0.00	0.05±0.01
Phenol	14.96	secondary	0.00	0.80±0.06	0.00	0.65±0.05
2-propenyl-Benzene	15.44	secondary	0.00	0.21±0.01	0.00	0.17±0.03
1-propenyl-Benzene	17.10	secondary	0.55±0.10	0.15±0.03	0.37±0.04	0.13±0.02
o/m/p-Cresol	17.45+18.18	secondary	0.00	1.19±0.14	0.00	0.94±0.11
Naphthalene	21.63	tertiary-PAH	2.34±0.21	0.24±0.06	2.58±0.34	0.17±0.03
2-methyl-Naphthalene	24.83	tertiary-alkyl	0.13±0.03	0.09±0.02	0.10±0.01	0.08±0.01
1-methyl-Naphthalene	24.26	tertiary-alkyl	0.09±0.02	0.07±0.02	0.08±0.01	0.05±0.01
Biphenyl	27.07	tertiary-PAH	0.09±0.01	0.03±0.03	0.12±0.01	0.00
Acenaphthylene	28.92	tertiary-PAH	0.76±0.04	0.06±0.01	0.90±0.12	0.03±0.01
Dibenzofuran	30.58	secondary	0.04±0.00	0.00	0.02±0.02	0.01±0.01
Fluorene	32.19	tertiary-PAH	0.19±0.03	0.06±0.01	0.14±0.02	0.06±0.01
Phenanthrene	36.48	tertiary-PAH	0.59±0.04	0.06±0.01	0.65±0.08	0.03±0.01
Anthracene	36.70	tertiary-PAH	0.14±0.02	0.01±0.01	0.15±0.02	0.00
Fluoranthene	40.89	tertiary-PAH	0.19±0.04	0.00	0.24±0.04	0.00
Pyrene	41.61	tertiary-PAH	0.23±0.05	0.00	0.31±0.06	0.00
Cyclopenta[cd]pyrene	45.41	tertiary-PAH	0.05±0.02	0.00	0.10±0.03	0.00
Benzo[a]anthracene	45.45	tertiary-PAH	0.03±0.01	0.00	0.06±0.01	0.00
Chrysene	45.57	tertiary-PAH	0.04±0.01	0.00	0.09±0.02	0.00
Secondary tar			5.16±0.71	4.49±0.32	4.86±0.52	4.04±0.48
Tertiary alkyl tar			0.31±0.05	0.18±0.05	0.29±0.01	0.13±0.02
Tertiary PAH tar			4.57±0.43	0.42±0.08	5.21±0.63	0.29±0.04
Total tar			10.04±1.19	5.08±0.43	10.37±1.13	4.47±0.51
Tar dew point* [˚C]			148.2	70.5	159.1	58.3

[a] According to Milne et al. [34] classification, * Obtained from the ECN tar dew point site (www.thersites.nl)